Experimental investigations of plasma perturbation in Thomson scattering applied to thermal plasma diagnostics

Krzysztof Dzierżęga* and Witold Zawadzki
Instytut Fizyki im. M. Smoluchowskiego, Uniwersytet Jagielloński, ulica Reymonta 4, 30-059 Kraków, Poland

Bartłomiej Pokrzywka
Obserwatorium Astronomiczne na Suhorze, Akademia Pedagogiczna, ulica Podchorążych 2, 30-459 Kraków, Poland

Stephane Pellerin
LASEP, Faculte des Sciences-Bourges, Université d'Orléans, BP 4043, 18028 Bourges Cedex, France
(Received 9 February 2006; published 25 August 2006)

Time and space resolved measurements of Thomson scattering of 532 nm, 6 ns laser pulses were performed on argon thermal discharge plasma with electron temperature $T_e > 10\,000$ K and electron density $8 \times 10^{22}\ \mathrm{m}^{-3} < n_e < 2 \times 10^{23}\ \mathrm{m}^{-3}$. From these measurements, variations of the electron density and temperature across the laser beam and their evolution during the laser pulse were determined. While the electron density is augmented by no more than a few percent the electron temperature is significantly increased along the axis of the laser beam due to laser heating. It is also shown that the higher initial electron density, the more disturbed is the plasma. The initial "undisturbed" electron density was derived by studying the spatial variations of n_e within the laser beam. On the other hand, the initial electron temperature was determined by studying the temporal evolution of T_e during the laser pulse and then by extrapolating the results to the origin of the pulse. Despite strong and nonlinear plasma heating by the Thomson scattered laser light, our study yields temperatures close to those obtained by modeling and time-resolved spectroscopic measurements.

DOI: 10.1103/PhysRevE.74.026404 PACS number(s): 52.70.Kz, 52.25.Os, 52.80.Mg

I. INTRODUCTION

Thomson scattering (TS) is a laser diagnostic technique commonly used for the measurement of local electron and ion temperatures and electron densities in a variety of laboratory and industrial plasmas. These parameters are derived by analyzing spectra of the scattered laser light.

Thomson scattering has played an important role in the studies of nuclear fusion plasmas where it is still the most reliable method for measurements of the electron temperature. TS has also been applied to investigate various kinds of glow discharge plasmas [1–5], laser-induced plasmas [6–9], pinch plasmas [10–12], but also to study thermal plasmas such as welding arcs and plasma jets [13–19].

Principal advantages of Thomson scattering are high spatial resolution and ease with which the measured data can be interpreted. The standard plasma parameters, the electron temperature and density can be directly derived from the electron feature of the TS spectrum without any assumptions about the plasma symmetry, equilibrium state or its chemical composition whereas plasma composition itself can be deduced from the ion feature [20–22].

On the other hand, due to very low cross section for the Thomson scattering and strong plasma radiation, the measurements require high-power pulsed lasers which may cause considerable perturbation of the plasma state. Such perturbation is negligible in nuclear fusion plasmas of high electron temperatures (T_e) at moderate laser intensities, i.e., below intensities at which anomalous absorption occurs (see Fig. 3 of Ref. [9]). Similarly, no disturbance is observed in the TS experiments in glow discharge plasmas of low electron densities (n_e). However, in the case of thermal plasma of simultaneously high n_e and low T_e application of even very low laser intensities may result in considerable electron heating by absorption of the laser light. The heating effect has been usually taken into account by measuring the electron temperature as a function of laser pulse energy and then by linear extrapolation of the results to zero pulse energy.

A number of TS measurements of electron and ion temperatures in atmospheric-pressure thermal plasmas have been performed over the last decade [14–16,18,19,23]. These measurements showed that T_e is higher than the ion temperature (T_i) by several thousands K in all plasma regions. Moreover, the excitation temperature determined with the use of spectroscopic measurements is in agreement with the ion temperature measured by TS. These observations are difficult to reconcile with the conclusions of most theoretical and experimental studies which indicate that the excitation temperature reflects the electron temperature and that the central regions of welding arcs and plasma jets are in, or close to, local thermal equilibrium (LTE).

The question of the thermal plasma perturbation by the pulsed laser in TS has recently been theoretically studied by Murphy [24,25]. He solved a one-dimensional equation for the electron heating in thermal argon plasma by absorption of radiation of a square, 7 ns long laser pulse taking into account such cooling processes as electron thermal conduction, energy transfer to heavy particles in inelastic and elastic collisions and radiative emission. These calculations show that the laser heating is a highly nonlinear function of the laser power. This is directly related to the strong temperature

*Electronic address: krzycho@netmail.if.uj.edu.pl

dependence of the absorption of the laser energy and the rates for the collisional and radiative cooling. Furthermore, the results of this theoretical model indicate that the linear extrapolation of T_e to zero laser energy overestimates the initial electron temperature.

The model of Murphy seems to explain the most salient issues of the electron heating in thermal plasma but it is based on several important simplifications. For example, 3D plasma is reduced to a 1D cylinder, the laser pulse is approximated by a square pulse and the plasma is described using the simplistic collisional-radiative model. Therefore, the results and conclusions of his work need careful experimental verification which is the main objective of the present work.

Another issue, also related to the electron heating, concerns derivation of the local (in time and space) T_e and n_e from the scattered spectra. Each TS spectrum measured in the experiment is usually a spatial average over the laser beam cross section and a time average over the laser pulse duration. Since, in the case of thermal plasmas, the TS spectrum has partially collective character, the resulting average TS spectrum is a very complex function of the local values of plasma parameters. Thus, when the electron heating takes place, determination of the undisturbed electron temperature requires appropriate setting of the experimental conditions and careful processing of the measured TS spectra in order to account for the averaging effects. The second objective of this research was to answer the question on the applicability of the Thomson scattering method for studying thermal plasmas, and to find a practical way of determination of the local values of T_e and n_e by analysis of the TS spectra.

II. THOMSON SCATTERING

TS is a process of scattering of photons on nonrelativistic free electrons. TS measures the fluctuations of the electron density copropagating and counterpropagating along the scattering wave vector

$$\mathbf{k} = \mathbf{k}_s - \mathbf{k}_L, \quad |\mathbf{k}| = 4\pi \sin(\theta/2)/\lambda_L, \tag{1}$$

where $\mathbf{k}_L$ and $\mathbf{k}_s$ are the wave vectors of the incident laser beam and the scattered light, respectively, λ_L is the laser wavelength while θ is the scattering angle (see Fig. 1).

The character (collective or noncollective) of TS is governed by the scattering parameter $\alpha \equiv 1/(k\lambda_D)$, where λ_D stands for the Debye length. The scattering is noncollective when $\alpha \ll 1$ and has a collective character for $\alpha \gg 1$.

Detailed discussion of the theory of TS is presented in several monographies [26–29]. We recall only the TS features that are most important for its application to study of the thermal plasmas.

The spectral distribution of the scattered photons is described by the spectral density function $S(\mathbf{k}, \Delta\omega)$ where the frequency shift $\Delta\omega = \omega - \omega_L$. This function takes on different shapes depending on α. In the case of thermal plasmas with $T_i \cong T_e \gtrsim 10\,000$ K and $n_e > 10^{22}$ m^{-3} and when the observation is carried out perpendicularly to the laser beam with $\lambda_L = 532$ nm, TS spectrum has a collective or partially collective character and is plotted in Fig. 2 for $\Delta\omega > 0$.

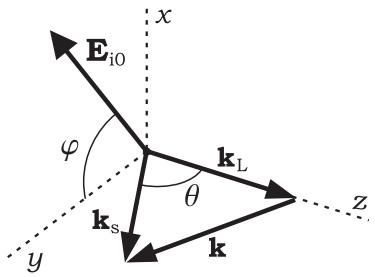

FIG. 1. Geometry of the Thomson scattering: $\mathbf{k}_L$ and $\mathbf{k}_s$ are the wave vectors of the incident laser beam and the scattered light, respectively, while $\mathbf{k} = \mathbf{k}_s - \mathbf{k}_L$ is the scattering wave vector. θ marks the scattering angle. The polarization of the incident laser beam is defined by angle φ between the scattering plane $(\mathbf{k}_s, \mathbf{k}_L)$ and laser field $\mathbf{E}_{i0}$.

The spectrum consists of a narrow ion feature, S_i near the laser frequency and much broader electron feature, S_e in the form of two satellites symmetrically separated from the laser frequency by $\Delta\omega_e = \pm(\omega_{p,e}^2 + 3k_B T_e k^2/m_e)^{1/2}$, where $\omega_{p,e} = [e^2 n_e/(\epsilon_0 m_e)]^{1/2}$ is the plasma frequency. Typically the ion contribution is almost two orders of magnitude narrower than the electron one in the frequency or wavelength domain so that they are almost completely separated. Resolution of the ion feature is very challenging because of its narrow width and overlap with the Rayleigh and stray-scattered laser light. In the frame of this work we concentrate only on S_e which is sufficient for derivation of the standard plasma parameters T_e and n_e. The ion feature will not be further considered.

Examples of the electron contribution to TS spectra are shown in Figs. 3(a) and 3(b) as calculated under typical conditions corresponding to thermal plasmas and to perpendicular observation $(\theta = \pi/2)$ of the light scattered of the incident laser beam at $\lambda_L = 532$ nm.

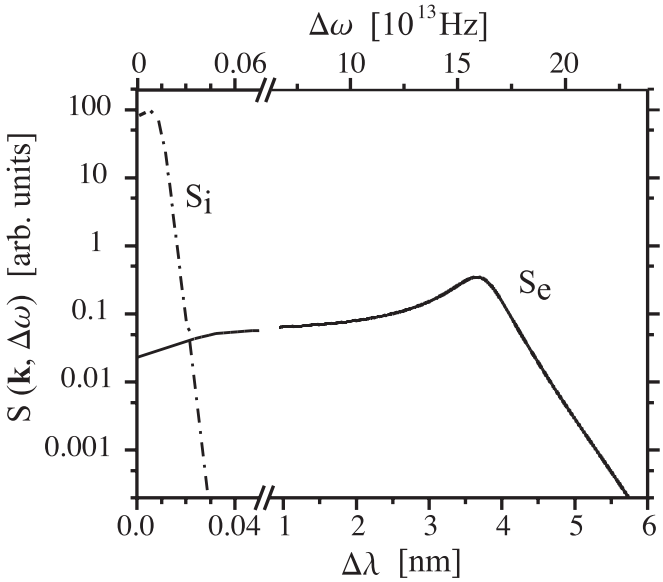

FIG. 2. Spectral density function of the Thomson scattering spectrum calculated according to [26] for $\lambda = 532$ nm, $\varphi = \theta = \pi/2$ and for $n_e = 1.0 \times 10^{23}$ m^{-3} and $T_e = 14\,500$ K.

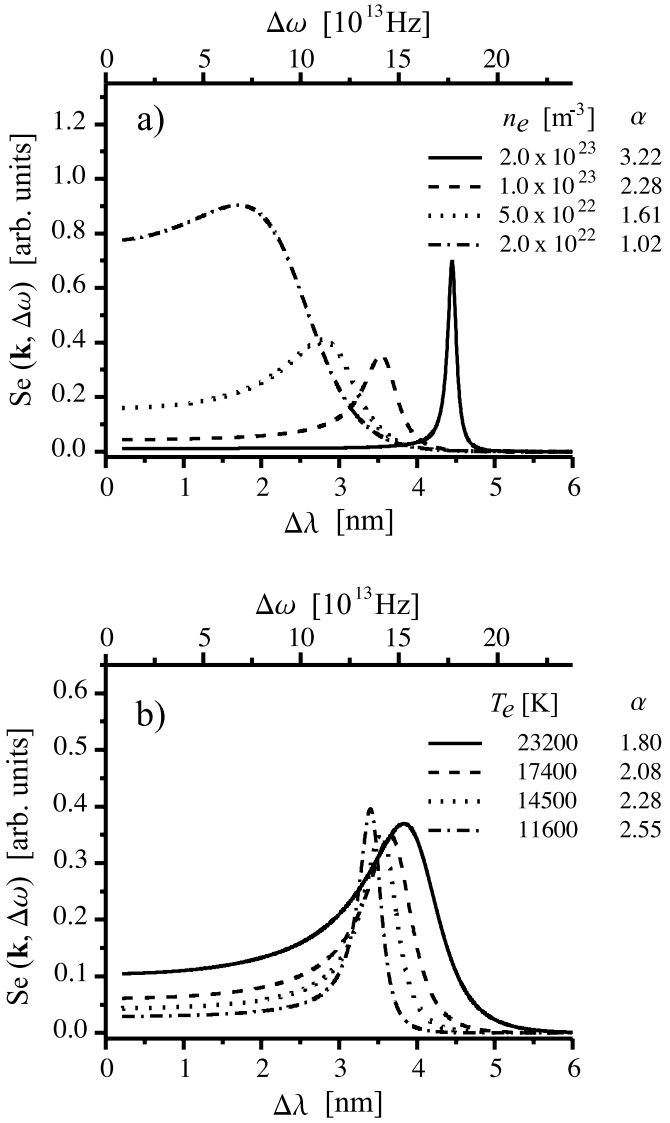

FIG. 3. Contributions of the electron term to the spectral density function in the Thomson scattering spectrum calculated for $\lambda_L = 532$ nm, $\varphi = \theta = \pi/2$ and for several values of α at (a) constant $T_e = 14\,500$ K and different n_e, (b) constant $n_e = 1.0 \times 10^{23}$ m^{-3} and different T_e.

The most characteristic for all of these spectra is the satellite peak which becomes more and more distinct with the increase of the scattering parameter α. In general, the shape of the satellite is determined by T_e whereas its separation from laser frequency is related to both T_e and n_e. These features of partially collective TS spectra enable one to independently determine both n_e and T_e without absolute calibration of the scattered power.

III. ELECTRON HEATING BY THE LASER PULSE

In typical experiments of TS in thermal plasmas such as welding arcs or plasma jets, a few nanosecond laser pulses with energies of the order of 10–200 mJ and at a repetition rate of about 10 Hz are used. The laser beam, usually at $\lambda_L = 532$ nm, is focued in the plasma region into the spot of a radius of about 200 μm. The scattered spectra are collected in the direction perpendicular to the laser beam and are integrated over duration of the laser pulse and summed up over the cross section of the laser beam.

The need of high laser powers in these experiments is caused not only by a very low scattering cross section for the TS process but also by the fact that TS signal has to compete with statistical fluctuations of the strong radiation background of thermal plasma. Unfortunately, high laser power can substantially perturb the plasma state by absorption of laser radiation. There are several absorption processes which might be considered; these are absorption at atomic transitions, single-photon and multiphoton ionization and inverse bremsstrahlung (IB). The first two processes mainly increase n_e while IB results in the electron heating and has been recognized as the principle absorption process of the laser light in the case of thermal plasmas [25].

Assuming the absence of any cooling channels, the upper limit for the laser-induced increase of T_e has commonly been evaluated as [26,29]

$$\frac{\Delta T_e}{T_e} = \frac{2}{3}\frac{\kappa_{\mathrm{IB}} E_L}{k_B T_e n_e \pi r_0^2}, \tag{2}$$

where E_L is the laser energy and r_0 is the laser beam radius in the plasma region. The absorption coefficient κ_{IB} for IB is given by

$$\kappa_{\mathrm{IB}} = \left(\frac{32\pi}{27}\right)^{1/2} \frac{\sum_Z Z^2}{m_e^2 c^2} \left(\frac{e^2}{4\pi\varepsilon_0}\right)^3 \frac{\lambda_L^3}{h} \left(\frac{m_e}{k_B T_e}\right)^{1/2} \times n_{i,Z} n_e [1 - \exp(-hc/k_B T_e \lambda_L)] \bar{g}_{ff}(\lambda_L), \tag{3}$$

where Z is the ion charge, $n_{i,Z}$ is the density of ions in the Zth ionization stage and $\bar{g}_{ff}$ denotes the Gaunt factor for free-free transitions. Substituting the absorption coefficient from Eq. (3) we can rewrite Eq. (2) as

$$\frac{\Delta T_e}{T_e} = 6.6 \times 10^{-5} \frac{\sum_Z Z^2 n_{i,Z}}{T_e^{3/2}} \frac{E_L}{\pi r_0^2} \times \bar{g}_{ff}(\lambda_L) \lambda_L^3 [1 - \exp(-hc/k_B T_e \lambda_L)]. \tag{4}$$

As a result, the total increase of T_e strongly depends on the transient electron temperature and density and hence the heating process is nonlinearly dependent on the laser pulse energy. An estimated evolution of the increase of T_e assuming $E_L = 100$ mJ, $r_0 = 200$ μm and the plasma close to LTE with initial $T_e = 17400$ K and $n_{i,1} \cong n_e = 2.0 \times 10^{23}$ m^{-3} is shown in Fig. 4 for the square 6 ns long laser pulse.

In the studied case, the upper limit for the final T_e (solid line) is found to surpass the initial value of T_e by about 150% but also to be much lower than the final T_e calculated assuming a constant value of κ_{IB} during the laser pulse (dotted line). Since the measured TS spectra are dominated by photons coming from the central part of the Gaussian laser pulse, the derived electron temperature $T_{e,\max}$ should correspond to the one at the maximum intensity of the laser pulse.

Hence, in Fig. 5 $T_{e,\max}$ denotes the electron temperature calculated for the time corresponding to the middle of the

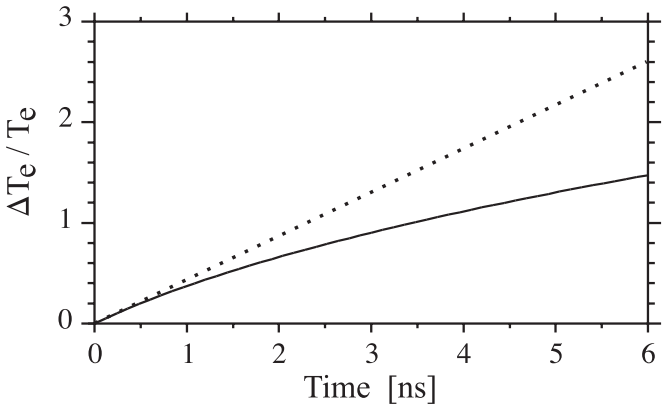

FIG. 4. Temporal evolution of the upper limit of the electron temperature increase during the laser pulse. Calculations were performed for the LTE plasma with initial T_e=17 400 K, $n_i \approx n_e$=2.0 $\times 10^{23}$ m^{-3} illuminated with the square laser pulse of energy of 100 mJ and of the diameter of 400 μm and assuming constant (dotted line) and temperature, i.e., time-dependent (solid line) κ_{IB}. Under such physical conditions $\bar{g}_{ff}(\lambda_L)$=1.2 according to Ref. [30].

laser pulse and is plotted as a function of the total laser energy. These figures indicate rapid increase of electron heating with increasing n_e [Fig. 5(a)] and decreasing the initial value of T_e [Fig. 5(b)]. Even without taking into count cooling processes the electron heating represented by $T_{e,\max}$ is strongly nonlinear function of the laser energy. It follows that a linear extrapolation of the experimental results to the zero pulse energy must overestimate the initial (unperturbed) electron temperature.

The model of electron heating by the laser pulse in argon thermal plasma that also includes simultaneous electron cooling has been recently published by Murphy [24,25]. Electrons heated by the laser pulse are cooled by: electron thermal conduction (ETC), energy transfer to heavy particles in elastic collisions (ETHP), electron-impact ionization (EII), and by radiative emission (RE) each of these processes being strongly dependent on T_e. Moreover, Murphy assumed a Gaussian spatial profile of the laser beam, a square temporal pulse shape, and equal initial temperatures of the heavy particles and electrons. The heating and cooling of electrons during the laser pulse is described by a one-dimensional energy conservation equation which in polar geometry takes the form

$$\frac{\partial}{\partial t}\left(\frac{5}{2}k_B n_e T_e\right) = \frac{1}{r}\frac{\partial}{\partial t}\left(r k_e \frac{\partial T_e}{\partial r}\right) + \frac{\kappa_{\mathrm{IB}} E_L}{A\tau_L} - W_{eh} - \sum_{i=1}^{2} R_i E_i - U, \tag{5}$$

where τ_L is the laser pulse duration, A is the cross-sectional area of the laser beam, r is the radial coordinate (r=0 corresponds to the center of the laser beam cross section) while k_e and U are the electron thermal conductivity and the radiative emission coefficient, respectively. $R_{1(2)}$ is the electron-impact ionization rate of neutral (singly ionized) argon atoms and $E_{1(2)}$ is their ionization energy. Finally, W_{eh} is the rate transfer of energy from electrons to heavy particles through elastic collisions which according to Ref. [31] is given by

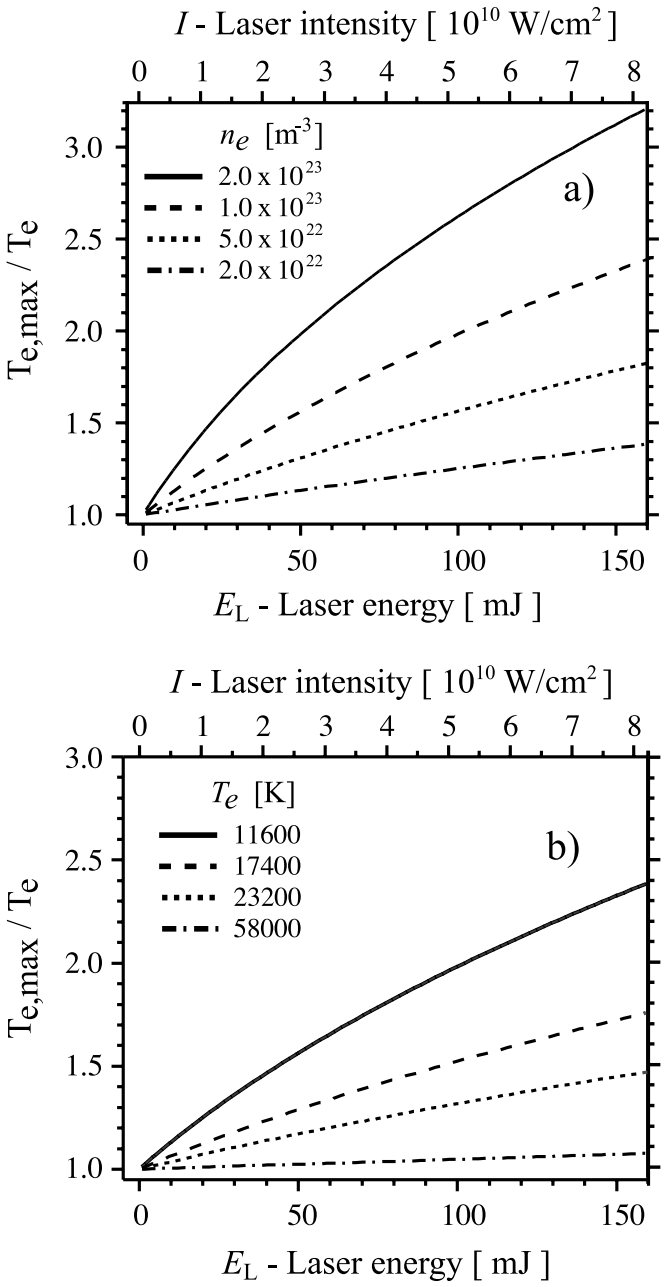

FIG. 5. Electron temperature ($T_{e,\max}$) calculated in the middle of the square 6 ns laser pulse for different total laser energies. (a) T_e =11600 K, (b) n_e=1.0$\times 10^{23}$ m^{-3}. In both cases n_i=n_e is assumed.

$$W_{eh} = 2\frac{m_e}{m_h}\frac{3}{2}k_B(T_e - T_i)n_e\nu_{eh}, \tag{6}$$

where m_e and m_h are the electron and heavy-particle masses while ν_{eh} denotes the electron-heavy-particle collision frequency.

Figure 6 shows results of this model for the evolution of T_e and densities of the plasma species during the laser pulse. In the same figure we added a plot depicting evolution of the electron temperature ($T_{e,h}$) as calculated according to Eq. (4) at the given physical conditions and without cooling channels.

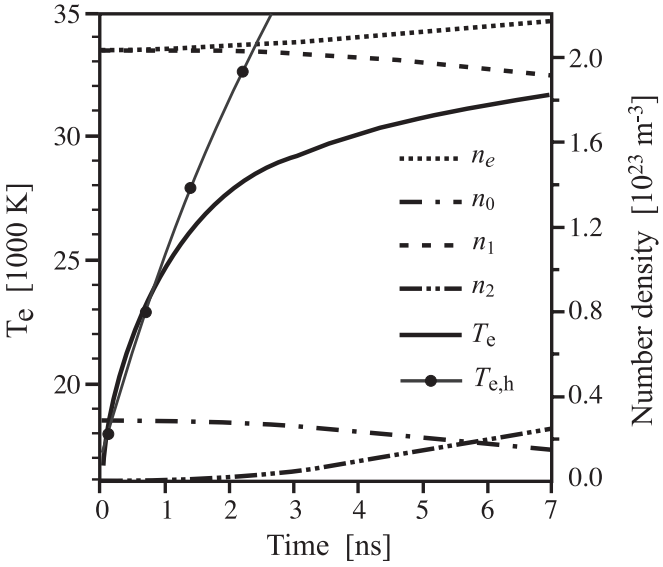

FIG. 6. Evolution of the electron temperature and density of the plasma species during the 7 ns laser pulse. The laser intensity is 4.5×10^{10} W/cm^2 and the initial electron temperature is 17 000 K. n_0, n_1, and n_2 denote the number densities of the neutral, singly ionized and doubly ionized atoms. These results are reproduced after Refs. [24,25]. $T_{e,h}$ is the electron temperature calculated according to Eq. (4) at given physical conditions.

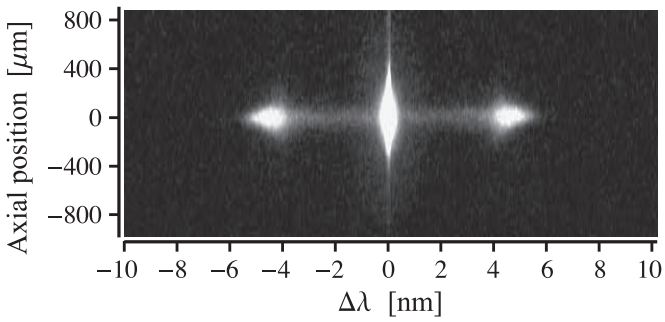

FIG. 7. An ICCD image of the TS spectrum. The position in this picture is measured along the z axis, and with respect to the center of the laser beam. The arc discharge was operated in pure argon and at the arc current $I=100$ A. The spectrum corresponds to the scattering off the axial region of the arc plasma and $z=4.0$ mm above the cathode tip. The image was integrated over 10 ns and averaged over 1000 laser shots. Laser intensity was 7.8×10^{10} W/cm^2.

It is evident that T_e rises most rapidly in the early stages of the laser pulse and after about 1 ns the heating rate considerably decreases. This results from increasing of the rate of energy loss through cooling processes and, to much lesser extent from lower absorption coefficient of laser radiation with increasing T_e. The rate of energy loss increases during the laser pulse which can be inferred from a growing discrepancy between the curves representing T_e and $T_{e,h}$ in Fig. 6. Out of four possible cooling processes the electron thermal conduction and energy transfer to heavy particles through electron impact ionization play the dominant role. For instance, the power losses per unit volume due to ETC and EII after 1 ns of laser illumination are of the order of 10^7 W/cm^3. These estimations were made for physical conditions given in Fig. 6 with the assumption that after 1 ns $T_e(r,t=1\text{ ns})=T_{e,h}(r,t=1\text{ ns})$.

All necessary coefficients were calculated as in Ref. [25]. The other two processes, i.e., ETHP and RE, are of minor importance as the related power losses are of the order of 10^5 W/cm^3 and 5×10^4 W/cm^3, respectively. In Fig. 6 one can also notice that while, at the end of the laser pulse, T_e is almost doubled, n_e is augmented only by about 5%. Such small scale of the n_e increase results from relatively long ionization times which are of the order of microseconds, in sharp contrast to the characteristic times for heating and cooling which are as short as a few nanoseconds [32,33]. The efficiency of this cooling process results from great amount of energy (>15.75 eV) transferred in single EII process rather than from the large number of created electrons.

Our theoretical considerations clearly imply that TS method used to study thermal plasmas inevitably leads to plasma perturbation predominantly in the form of electron heating. The plasma is disturbed to different extent depending on the laser energy, the position within the laser beam and the time instant during the laser pulse.

IV. EXPERIMENT

All details concerning the plasma generator can be found in Refs. [34,35]. In general, the arc discharge was generated from a conical cathode tip (cone angle of 60°) made of a 2-mm diameter, thoriated (2%) tungsten rod surrounded by a water-cooled nozzle. The upper part of the arc consists of two copper discs with a 5 mm channel diameter. The first disc served to improve the arc stability, whereas the second disc was used as an anode. The distance between the cathode tip and the first disc was about 9 mm. The arc was operated at atmospheric pressure in pure argon (99.995 %) with a flow rate of 4 l/min and in the current range of 80–100 A.

In the TS experiment we used a vertically polarized ($\varphi=\pi/2$) second harmonic ($\lambda_L=532$ nm) of a Nd:YAG laser which delivered laser pulses of energies up to 200 mJ and of about 6 ns duration. The beam was passing through the laser power attenuator and then it was focused to the spot with the diameter of about 300 μm on the plasma axis and a few millimeters above the cathode tip. The distance between the cathode and the laser beam was varied by lowering or lifting the table of the arc generator. The scattered light was collected at an angle $\theta=79.5°$.

The investigated plasma was imaged onto the entrance slit of a spectrograph (1.6 nm/mm reciprocal dispersion) with an enlargement factor equal to 1. The width of the slit was set to 20 μm. The TS spectra were collected over the wavelength range of 521.9–542.1 nm. In order to improve a signal-to-noise ratio only a vertically polarized signal was considered by inserting the polarizer in the path of the scattered light. Single-shot scattering spectra were measured using a gated two-dimensional intensified charge-coupled device (ICCD) camera and averaged over 1000 shots. The TS spectra shown in Fig. 7 were obtained by subtracting the spectra collected with and without the laser beam. The spectral and spatial resolution were found to be 0.032 nm and 19 μm, respec-

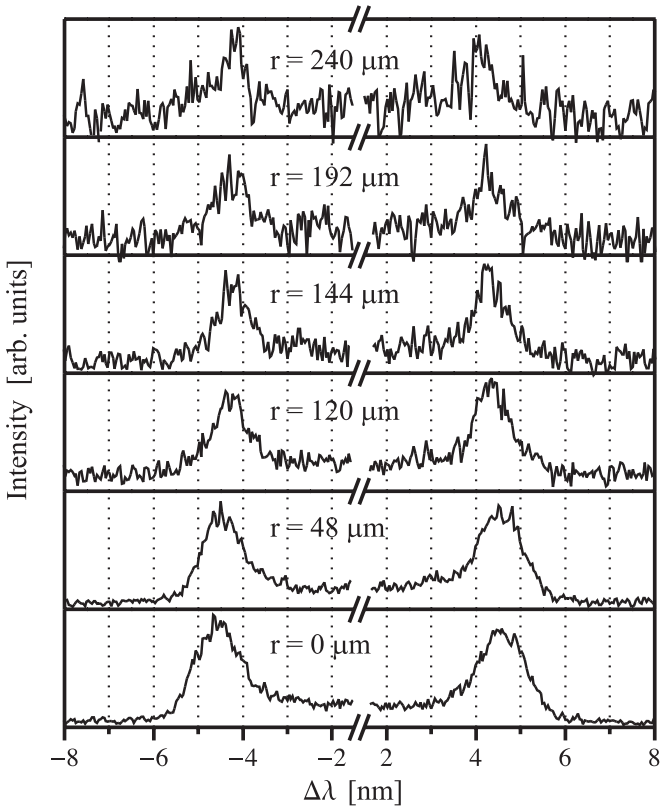

FIG. 8. Example of the TS spectra (electron terms) obtained from different plasma regions across the laser beam. The spectra obtained at the same experimental conditions as in Fig. 7. The position indication in the figures is relative to center of the laser beam. Spatial resolution $\Delta r = 22\ \mu$m.

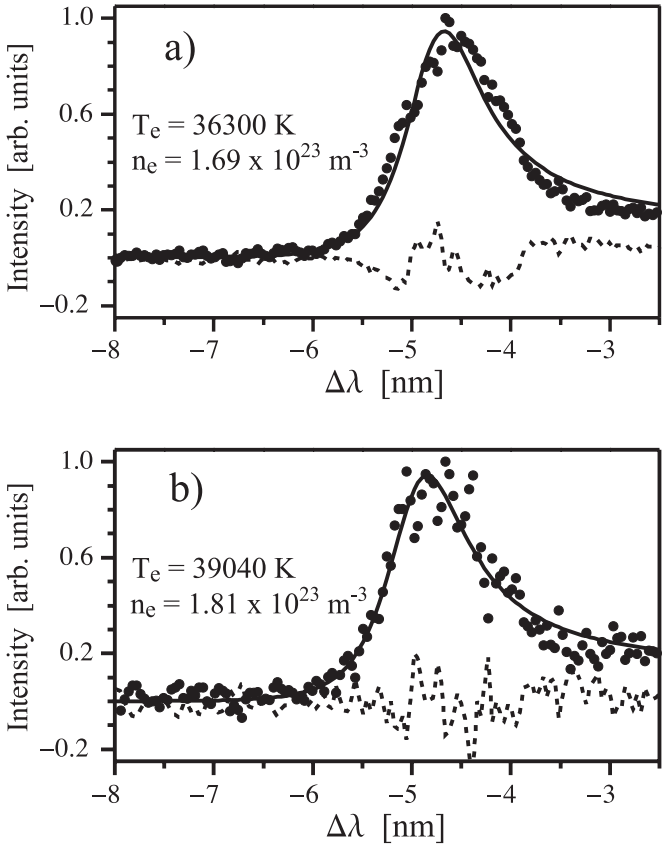

FIG. 9. Example of (a) measured and (b) Abel inverted TS spectra. Measurements carried out under experimental conditions depicted in Fig. 7. The spectrum (a) corresponds to the one at the center of the laser beam, $r=0$. Full lines represent the fitted TS spectra, the dashed lines are the residuals.

tively. The camera was synchronized to the laser pulse with variable delay in order to study the temporal evolution of the TS spectra with the laser pulse. The time resolution was 2.5 ns, being mainly limited by the gate width of the camera.

V. RESULTS AND DISCUSSION

A typical image of the TS spectrum registered by the ICCD camera is shown in Fig. 7. Apart from the TS light, the central part of this spectrum contains also the Rayleigh scattered light, as well as the stray light. This part of the spectrum was discarded from further analysis. The collected spectra extend spatially over a few hundreds of microns which enables to investigate them at different positions across the laser beam and such vertically resolved spectra are shown in Fig. 8.

These figures clearly reveal that TS spectrum changes within the laser beam. In general, the maxima shift away and become broader while approaching the center ($r=0\ \mu$m) of the beam cross section. This spatial variation is a direct indication of the plasma perturbation by laser radiation assuming that the plasma is initially homogeneous across the interaction volume. The validity of this assumption is confirmed by the spatial symmetry of the measured spectra with respect to the center of the laser beam.

A. Spatially resolved n_e and T_e within the laser beam

The registered spectra presented in Fig. 8 are laterally integrated across the laser beam. The local, radially resolved spectra, were obtained assuming the cylindrical symmetry of the laser beam and applying the Abel transformation procedure pixel by pixel as it is described in Ref. [36]. The local electron densities and temperatures were then obtained by fitting the spectral density function $S(\mathbf{k},\Delta\omega)$ to the Abel inverted spectra.

Figures 9 present the TS spectra obtained for the center of the laser beam before (a) and after (b) the Abel transformation procedure together with the fitted theoretical spectra and their residuals. The measurements were carried out under experimental conditions specified in the caption to Fig. 7. The values for n_e and T_e obtained from the fit are shown in the figures. The residuals of the fitted curves suggest that while the statistical errors dominate in the case of the Abel inverted spectra, the systematic errors are dominant in the case of noninverted spectra. Moreover, the differences between the n_e and T_e values derived from the measured and Abel inverted spectra are greater than the estimated uncertainties. It follows that application of the Abel transformation is essential for correct interpretation of the registered data.

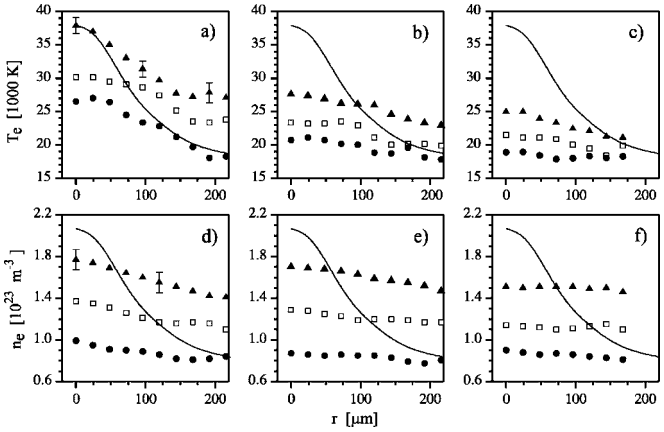

FIG. 10. Local values of T_e (a)–(c) and n_e (d)–(f) derived from the Abel inverted TS spectra. Measurements carried out for the laser pulse energy of 150 mJ (a),(d), 50 mJ (b),(e), and 20 mJ (c),(f) and for the following discharge conditions: (△) $I=100$ A, $z=4.0$ mm above the cathode, (□) $I=100$ A, $z=6.0$ mm and (●) $I=80$ A, $z=6.5$ mm. The full lines indicate intensity distribution across the laser beam.

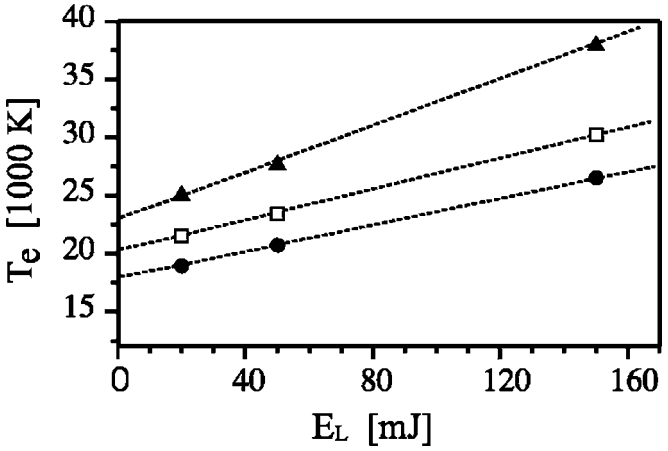

FIG. 11. A linear extrapolation (the dotted lines) to zero pulse energy of the electron temperatures derived at the center of the laser beam ($r=0$ μm) from the Abel inverted TS spectra. (▲) $I=100$ A, $z=4.0$ mm, (□) $I=100$ A, $z=6.0$ mm, and (●) $I=80$ A, $z=6.5$ mm.

The results of our experimental studies on TS are summarized in Figs. 10(a)–10(f). These figures present the results of the measurements performed at laser energies of 150, 50, and 20 mJ and for different initial conditions of the plasma. The latter were realized by changing the arc current, the plasma region or both. Usually, with lower discharge current and increasing distance from the cathode we expect lower values for n_e and T_e. The TS data measured at laser energies lower than 20 mJ were already too noisy to be spatially analyzed, and the TS signal vanished at energies below 10 mJ.

Figures 10(a)–10(c) show that T_e increases with approaching the center of the laser beam and to some extent the same occurs for the electron density except the case of the lowest pulse energy. It is evident that variations of T_e and n_e are dependent not only on the pulse energy but also on the initial plasma conditions. In general, the higher n_e the higher increase of T_e is observed, which is due to the rapid increase of the absorption coefficient of laser radiation with n_e. Regardless of the initial plasma conditions, no increase of n_e (within the uncertainty limits) is observed at energy of 20 mJ [Fig. 10(f)]. The spatially averaged electron densities derived at this energy are $1.50(6)\times10^{23}$ (▲), $1.12(2)\times10^{23}$ (□), and $0.86(2)\times10^{23}$ (●) m^{-3}. These results are consistent with n_e determined on the wing ($r>150$ μm) of the laser beam at pulse energies of 50 and 150 mJ and they correspond to the initial undisturbed n_e of the investigated plasmas. If we assume the studied plasmas to be in the LTE state then at the given electron densities the corresponding electron temperatures $T_{e,\mathrm{LTE}}$ should be equal to 13 950 (▲), 13 100 (□), and 12 500 (●) K (kelvins) [37].

In the TS experiments in thermal plasmas the electron heating effect has been usually taken into account by linear extrapolation of the results obtained at different pulse energies to zero energy. However, as it has already been discussed in the previous section, such method inevitably yields higher electron temperature than the undisturbed one. The results of the extrapolation of T_e determined in our experiments at the center ($r=0$ μm) of the laser beam under given plasma conditions are presented in Fig. 11.

The resulting "undisturbed" T_e are found to be 22 780 (▲), 20 090 (□), and 17 760 K (●) and they are much higher than the electron temperatures $T_{e,\mathrm{LTE}}$ corresponding to the LTE argon plasmas.

B. Temporal evolution of n_e and T_e during the laser pulse

Temporal evolution of the plasma parameters (n_e and T_e) during the laser pulse was determined by measuring the time-resolved TS spectra. For this sake, the gate width of the ICCD camera was set to the smallest possible value of 2.5 ns and its trigger was delayed with respect to the laser pulse. After each measurement, three central pixels of the image of the scattered spectrum were grouped in the spatial direction for each of the spectral position. An example of such TS spectra recorded at different time delays Δt is plotted in Fig. 12. These spectra were measured for laser energy of 150 mJ, discharge current 100 A and by collecting the scattered light from the plasma spot 4.0 mm above the cathode.

The recordings corresponding to different Δt exhibit changes of the spectra. In addition to different intensities there is change in the observed shapes of the TS spectra, predominantly in the first stages of the laser pulse. This is another irrefutable evidence for the plasma perturbation by the laser pulse at given experimental conditions.

The temporal evolution of plasma parameters was studied by fitting the TS spectra to the time-resolved spectra and Figs. 13(a)–13(f) present compilation of the results. The measurements were performed at similar experimental conditions as for the spatial distributions of n_e and T_e.

Figures 13(d)–13(f) show that during the laser pulse the electron density is considerably elevated only in the case of the highest pulse energy. Again, no significant variations of n_e are observed during the laser pulse of energy of 20 mJ.

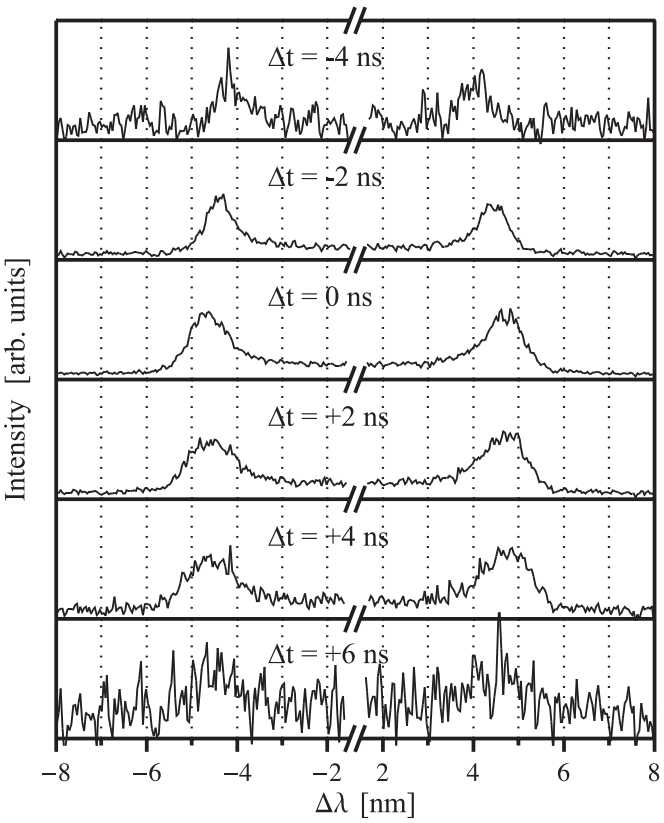

FIG. 12. An example of the TS spectra (electron terms) recorded at different delay times Δt. Δt=0 ns corresponds to the maximum of the laser pulse. The spectra obtained at experimental conditions as indicated in Fig. 7. Temporal resolution is 2.5 ns.

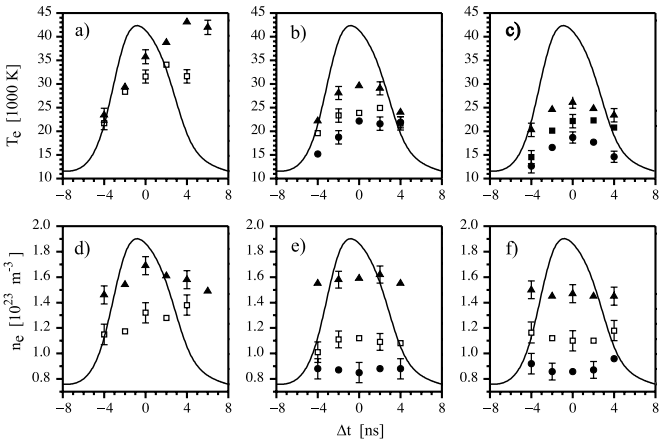

FIG. 13. Temporal evolution of the plasma parameters. Measurements carried out for the laser pulse energies of 150 mJ (a),(d), 50 mJ (b),(e) and 20 mJ (c),(f) and for the following arc currents and distances from the cathode tip: 100 A, 4.0 mm (▲), 100 A, 6.0 mm (□), and 80 A and 6.5 mm (●). Full lines indicate temporal distribution of the laser beam intensity.

The average electron densities determined in this case amount to $1.46(3)\times10^{23}$, (▲) $1.14(2)\times10^{23}$ (□), and $0.89(2)\times10^{23}$ (●) m^{-3} and they are consistent with the n_e values obtained from the spatially resolved TS spectra. It follows that, since neither spatial nor time variations of n_e are observed at the lowest applied energy, the laser pulse has none, or insignificant, impact on n_e and these values can be considered as the initial n_e.

Unlike n_e, T_e rapidly increases after switching on the laser pulse and it increases even at the lowest energy as it is evident from Figs. 13(a)–13(c). The rate of the heating depends on both the pulse energy and the initial plasma conditions. Again, the higher initial n_e the higher absorption coefficient of laser radiation and hence the higher increase of T_e. This effect is the most pronounced at the highest laser intensity [see Fig. 13(a)].

Basing on our theoretical considerations on the electron heating by laser radiation it is reasonable to approximate that the increase of T_e in the early stage of the laser pulse is linear with time. Such approach is especially justified for high laser energies, since then, at the early stages of the pulse, the rate of electron heating greatly dominates over the rate of cooling. Assuming such a linear increase of T_e in time, we extrapolated the results (up to Δt=0 ns) obtained at the highest laser energy to the origin ($\Delta t \approx -7$ ns) of the laser pulse. This extrapolation yielded the initial T_e of 14 000 (▲), 11 900 (□), and 10 000 (●) K, where the latter was obtained based on the results derived at energy of 50 mJ. Although the initial T_e estimated this way are of large uncertainty due to very limited temporal resolution of the experiment, they were found to be very close to the expected ones at given initial electron densities under assumptions of the LTE plasma conditions.

VI. SUMMARY AND CONCLUSIONS

In this work the method of Thomson scattering was investigated theoretically and experimentally in terms of its applicability to thermal plasmas. In particular, plasma perturbation by the laser radiation and the credibility of the results were studied. Time or space resolved TS measurements were performed on atmospheric-pressure argon arc plasmas at different energies of the laser pulse. From these measurements, the electron density and temperature variations across the laser beam and their evolution in time of the laser pulse were determined. The electron density is considerably affected only in the case of the strongest laser pulse energies applied. Unlike the electron density, the electron temperature is significantly disturbed even by the pulse of the lowest energy. The increase of the electron temperature is strongly dependent on both the particular position within the laser beam and the time instant during the laser pulse. Furthermore, the results of our experiment clearly show that the degree of plasma perturbation depends on the initial values of the plasma parameters. The higher initial electron density, the more disturbed is the plasma. The initial "undisturbed" electron density can be easily derived by studying the spatial variations of n_e within the laser beam mainly with the laser pulses of low energy. On the other hand, the initial electron temperature can be determined by studying temporal evolution of T_e during the laser pulse of high energy and then by extrapolating the results for the early stage of the pulse to the

origin of the pulse. The results of our experiment strongly support the results of the theoretical model presented in Refs. [24,25]. Our investigations additionally indicate that if TS data are properly analyzed they do not give evidence that such kind of thermal plasma is far from LTE.

ACKNOWLEDGMENTS

K.D wishes to acknowledge the partial support of this work by the Polish Ministry of Scientific Research and Information Technology Grant No. 1PO3B09026 and by project d'Action Intégreés—Polonium 6197.I/2005.

[1] H. J. Wesseling, and B. Kronast, J. Phys. D **29**, 1035 (1996).
[2] J. M. de Regt, R. A. H. Engeln, F. P. J. de Groote, and J. A. M. van der Mullen, Rev. Sci. Instrum. **66**, 3228 (1995).
[3] M. Huang and G. M. Hieftje, Spectrochim. Acta, Part B **40**, 1387 (1985).
[4] M. D. Bowden, T. Okamoto, F. Kimura, K. Uchino, K. Muraoka, T. Sakoda, M. Maeda, Y. Manabe, M. Kitagawa, and T. Kimura, J. Appl. Phys. **73**, 2732 (1993).
[5] T. Sakoda, H. Iwamiya, K. Uchino, K. Muraoka, M. Itoh, and T. Uchida, Jpn. J. Appl. Phys. **36**, L67 (1997).
[6] S. H. Glenzer, C. A. Back, K. G. Estabrook, R. K. Kirkwood, R. Wallace, B. J. MacGowan, B. A. Hammel, R. E. Cid, and J. S. DeGroot, Rev. Sci. Instrum. **68**, 97 (1997).
[7] J. Zheng, C. X. Yu, and Z. J. Zheng, Phys. Plasmas **4**, 2736 (1997).
[8] E. R. Kieft, J. J. A. M. van der Mullen, G. M. W. Kroesen, V. Banine, and K. N. Koshelev, Phys. Rev. E **70**, 056413 (2004).
[9] S. H. Glenzer, W. Rozmus, V. Yu. Bychenkov, J. D. Moody, J. Albritton, R. L. Berger, A. Brantov, M. E. Foord, B. J. MacGowan, R. K. Kirkwood, H. A. Baldis, and E. A. Williams, Phys. Rev. Lett. **88**, 235002 (2002).
[10] E. Fünfer, B. Kronast, and H. J. Kunze, Phys. Lett. **5**, 125 (1963).
[11] H. J. Kunze, E. Fünfer, B. Kronast, and W. H. Kegel, Phys. Lett. **11**, 42 (1964).
[12] T. Wrubel, S. Büscher, and H. J. Kunze, Plasma Phys. Controlled Fusion **42**, 519 (2000).
[13] A. W. DeSilva, D. E. Evans, and J. M. Forrest, Nature (London) **203**, 1321 (1964).
[14] S. C. Snyder, G. D. Lassahn, and L. D. Reynolds, Phys. Rev. E **48**, 4124 (1993).
[15] R. E Bentley, J. Phys. D **30**, 2880 (1997).
[16] S. C. Snyder, D. M. Crawford, and J. R. Fincke, Phys. Rev. E **61**, 1920 (2000).
[17] J. Jonkers, J. M. deRegt, J. A. M. van der Mullen, H. P. C. Vos, F. P. J. de Groote, and E. A. H. Timmermans, Spectrochim. Acta, Part B **51**, 1385 (1996).
[18] G. Gregori, J. Schein, P. Schwendinger, U. Kortshagen, J. Heberlein, and E. Pfender, Phys. Rev. E **59**, 2286 (1999).
[19] G. Gregori, U. Kortshagen, J. Heberlein, and E. Pfender, Phys. Rev. E **65**, 046411 (2002).
[20] A. W. DeSilva, T. J. Baig, I. Olivares, and H. J. Kunze, Phys. Fluids B **4**, 458 (1992).
[21] S. H. Glenzer, C. A. Back, K. G. Estabrook, R. Wallace, K. Baker, B. J. MacGowan, B. A. Hammel, R. E. Cid, and J. S. DeGroot, Phys. Rev. Lett. **77**, 1496 (1996).
[22] S. H. Glenzer, W. Rozmus, B. J. MacGowan, K. G. Estabrook, J. D. De Groot, G. B. Zimmerman, H. A. Baldis, J. A. Harte, R. W. Lee, E. A. Williams, and B. G. Wilson, Phys. Rev. Lett. **82**, 97 (1999).
[23] M. Tanaka and M. Ushio, J. Phys. D **32**, 1153 (1999).
[24] A. B. Murphy, Phys. Rev. Lett. **89**, 025002 (2002).
[25] A. B. Murphy, Phys. Rev. E **69**, 016408 (2004).
[26] O. E. Evans, and J. Katzenstein, Rep. Prog. Phys. **32**, 207 (1969).
[27] J. Sheffield, *Plasma Scattering of Electromagnetic Radiation* (Academic, London, 1975).
[28] I. H. Hutchinson, *Principles of Plasma Diagnostics* (Cambridge Academic Press, Cambridge, 2002).
[29] H. J. Kunze, in *Plasma Diagnostics* (North-Holland, Amsterdam, 1968).
[30] W. J. Karzas and R. Later, Astrophys. J., Suppl. Ser. **6**, 167 (1961).
[31] V. M. Lelevkin, D. K. Otorbaev, and D. C. Schram, *Physics of Non-Equilibrium Plasmas* (North-Holland, Amsterdam, 1992).
[32] S. Pellerin, B. Pokrzywka, K. Musioł, and J. Chapelle, J. Phys. (Paris) **5**, 2029 (1995).
[33] H. R. Griem, *Plasma Spectroscopy* (McGraw Hill, New York 1964).
[34] K. Dzierżęga, Ł. Bratasz, S. Pellerin, B. Pokrzywka, and K. Musioł, Phys. Scr. **67**, 52 (2003).
[35] B. Pokrzywka, K. Musioł, S. Pellerin, E. Pawelec, and J. Chapelle, J. Phys. D **29**, 2644 (1996).
[36] S. Pellerin, K. Musioł, B. Pokrzywka, and J. Chapelle, J. Phys. D **27**, 522 (1994).
[37] B. Pokrzywka, *Równowagowe i Spektroskopowe Własności Plazmy w Sąsiedztwie Katody Łuku Elektrycznego* (Wydawnictwo Naukowe Akademii Pedagogicznej, Kraków 2003) [in Polish].